

Article

Development of a Hydrogen Fuel Cell Prototype Vehicle Supported by Artificial Intelligence for Green Urban Transport

Krisztián Kun ^{1,*}, Lóránt Szabó ¹, Erika Varga ² and Dávid István Kis ³

¹ Department of Innovative Vehicles and Materials, GAMF Faculty of Mechanical Engineering and Computer Science, John von Neumann University, H-6000 Kecskemét, Hungary; szabo.lorant@nje.hu

² Hydrogen Technology Research Center, John von Neumann University, H-6000 Kecskemét, Hungary; varga.erika@nje.hu

³ Department of Automotive Technologies, Faculty of Transportation Engineering and Vehicle Engineering, Budapest University of Technology and Economics, Műegyetem rkp. 3, H-1111 Budapest, Hungary; kis.david@nje.hu

* Correspondence: kun.krisztian@nje.hu

Abstract: In the automotive sector, the zero emissions area has been dominated by battery electric vehicles. However, prospective users cite charging times, large batteries, and the deployment of charging stations as a counter-argument. Hydrogen will offer a solution to these areas, in the future. This research focuses on the development of a prototype three-wheeled vehicle that is named Neumann H2. It integrates state-of-the-art energy storage systems, demonstrating the benefits of solar-, battery-, and hydrogen-powered drives. Of crucial importance for the R&D platform is the system's ability to record its internal states in a time-synchronous format, providing valuable data for researchers and developers. Given that the platform is equipped with the ROS2 Open-Source interface, the data are recorded in a standardized format. Energy management is supported by artificial intelligence of the "Reinforcement Learning" type, which selects the optimal energy source for operation based on different layers of high-fidelity maps. In addition to powertrain control, the vehicle also uses artificial intelligence to detect the environment. The vehicle's environment-sensing system is essentially designed to detect, distinguish, and select environmental elements through image segmentation using camera images and then to provide feedback to the user via displays.

Keywords: hydrogen prototype; system modeling; environment detection



Citation: Kun, K.; Szabó, L.; Varga, E.; Kis, D.I. Development of a Hydrogen Fuel Cell Prototype Vehicle Supported by Artificial Intelligence for Green Urban Transport. *Energies* **2024**, *17*, 1519. <https://doi.org/10.3390/en17071519>

Academic Editor: Ning Zhao

Received: 24 February 2024

Revised: 16 March 2024

Accepted: 18 March 2024

Published: 22 March 2024



Copyright: © 2024 by the authors. Licensee MDPI, Basel, Switzerland. This article is an open access article distributed under the terms and conditions of the Creative Commons Attribution (CC BY) license (<https://creativecommons.org/licenses/by/4.0/>).

1. Background

The utilization of fossil fuels rules the world trend of energy supply, thanks to their multiple advantages, as follows: high energy density, availability, mature technology, and affordable costs. Nowadays, transport requires 27% of the total energy consumption [1], where 95% is covered with fossil fuels [2]. Transport, however, is responsible for about 22% of the CO₂ emissions, 30% of NO_x emissions, and 12% of total particulate matter emissions; thus, this sector can be a strategic intervention point in climate politics [3,4]. Although replacement of diesel and gasoline in mobility is certainly challenging [5,6] due to the consumption of over 70% of the total oil quantity in this field and the low number of appropriate candidates, it has to be noted that fossil fuels are widely used in other sectors, too (33% in transport, 27% in electricity production, 26% in industry, 8% in residential applications, and 6% in commercial use (Figure 1a)), the conversion of which is also demanding [7]. In addition to the environmental and economic issues, the energy transition is a political topic, as the rapidly depleting fossil fuel reserves are located unevenly across the planet [8,9].

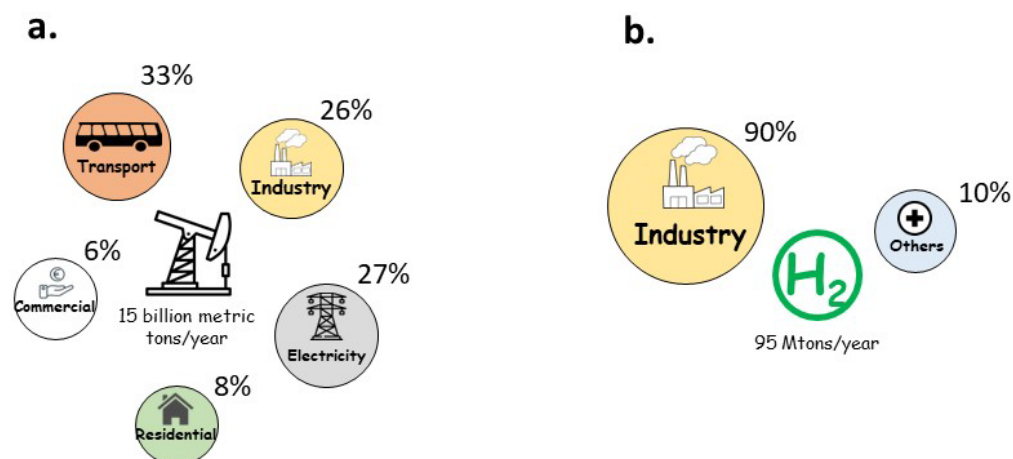


Figure 1. Current applications of fossil fuels (a) and hydrogen (b). Data were adopted from [1,10].

Hydrogen can be a solution for the abovementioned problems; it has the highest Higher Heating Value (HHV) in MJ/kg of all the fuels and the product of its combustion is only water, which makes it favorable in different areas such as transport, energy storage, electricity production, and residential applications [9,11]. Hydrogen and its compounds are abundant on Earth and its utilization has the lowest environmental impacts when it is extracted from renewable raw materials using renewable energy sources, such as water electrolysis [12]. Hydrogen has a lot of potential as an energy carrier; however, its role in transport is negligible today (Figure 1b). Worldwide, approximately 90% of industrial hydrogen is produced for the chemical industry; up to 50% for ammonia synthesis; and up to 40% for the petrochemistry, with some contribution for methanol synthesis; and the remaining 10% is used in miscellaneous fields, in electronics, plastics, metallurgy, food, and edible oil production lines [10]. In 2022, global hydrogen use reached 95 Mt of hydrogen [13], of which close to 50% was obtained through Steam Methane Reforming (SMR), resulting in so-called grey or blue hydrogen, while green hydrogen represents only 4% [14]. In 2030, the annual production of low-emission hydrogen is expected to reach 38 Mt [13], in which the following two groups of tasks play an essential role: scaling-up low-emission hydrogen production and increasing the use of hydrogen in sectors including heat and power generation, transport, and hard-to-decarbonize areas such as steel and cement production [15].

In mobility, hydrogen can be utilized either in modified internal combustion engines (ICEs) or fuel cells (FCs); however, the technical feasibility and interest in hydrogen FC vehicles (FCVs) significantly overweighs that of the hydrogen-powered ICE vehicles [11,16,17].

While the vehicle efficiency of diesel, gasoline, and compressed natural gas (CNG) ICE vehicles is only 14–17%, battery electric vehicles (BEVs) and FCVs exceed 25%; however, the well-to-wheel efficiency depends strongly on the power-to-H₂ process [11]. BEVs are another possible low-emission alternate to fossil fuel ICE vehicles and are reported to be more effective than FCVs (Figure 2). Currently, both technologies are affected by the high costs, limited service life, lack of appropriate charging infrastructure, and restricted availability of key raw materials; however, significant advantages of FCVs are unmodified consumer behavior and driving range, even in the case of vans; short refueling time; and stable operation at both high and low temperatures [18].

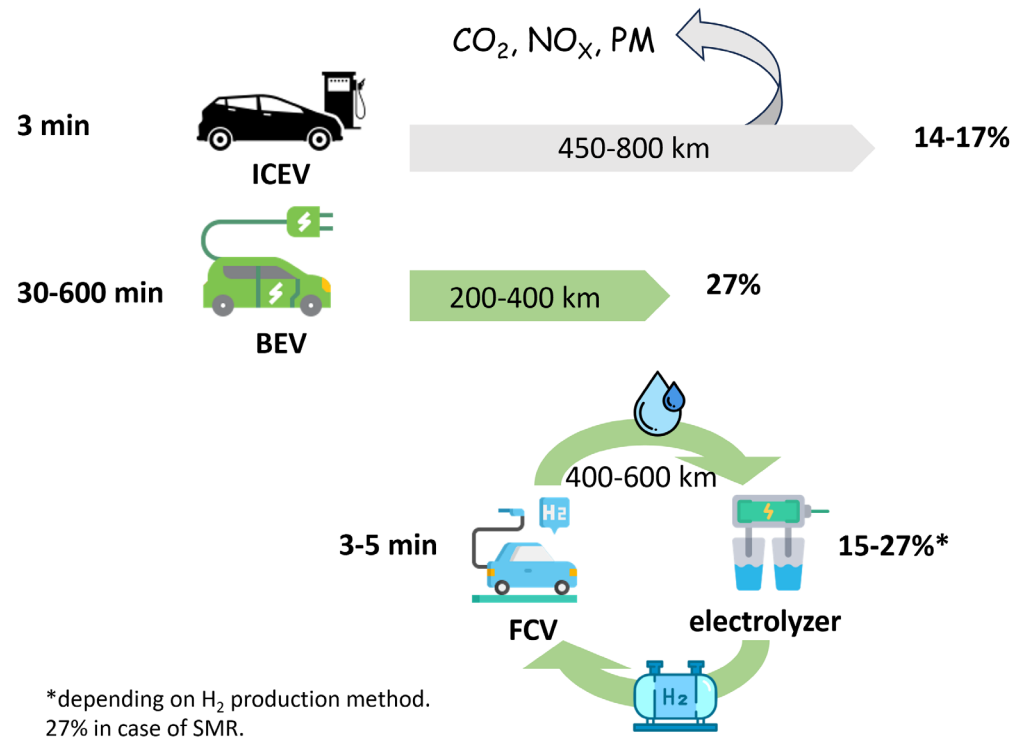


Figure 2. Recharging time, range, emissions, and well-to-wheel efficiencies of ICEVs, BEVs, and FCVs. Data were adopted from [11,19].

Nowadays, all the leading automotive companies have their own fuel cell programs, in which Toyota, Hyundai, and Honda have taken the main role [20]. Some companies, e.g., Daimler, Skoda, Volvo Buses, Solaris, have been introducing fuel cell electric buses in recent years [21] and fuel cell trucks have been developed by, among others, Scania, VDL Bus and Coach, Hyundai, and Nikola [22]. The implementation of FCVs is supported and coordinated by national and transnational projects, such as CUTE (Clean Urban Transport for Europe), JIVE, and JIVE2 (Joint Initiative for Hydrogen Vehicles across Europe) [16,23,24]. However, due to their earlier implementation, BEVs and plug-in hybrid electric cars gained a two orders of magnitude advance over FCVs regarding commercial production and their number reached 25 million in 2022 [25]. Being aware that a smart combination of green powertrain and energy storage technologies will result in enhanced efficiency and reliability [26], in our study, we provide a solution for a solar panel–battery–hydrogen FC energy system. It is expected that through the synergic combination with a mature (BEVs), an underdeveloped (solar vehicles), and an up-and-coming (AI) technology, a powerful FCV type can be constructed, which opens new pathways for the spread of climate-friendly vehicles.

Fuel cell hybrid electric vehicles (FCHEVs), which use batteries and/or ultracapacitors as auxiliary energy sources to supply excess energy and smooth the power demand fluctuation of the fuel cell, are of interest thanks to their enhanced efficiency and driving range [27–29]. In order to decrease hydrogen/energy consumption and extend the lifetime of the fuel cell, energy management systems (EMSs) are integrated that distribute the power load among the energy sources and can be classified as ruled-based, optimization-based, and learning-based EMSs. Recently, with the gaining attention of artificial intelligence (AI) and the internet of vehicles (IOV), interest in learning-based and cycle information-based EMSs has increased, with a prominent position of research on driving pattern recognition [30,31].

With a strong connection to BEVs, the concept of solar vehicles also exists, where solar energy is converted into electricity by solar panels and then electrical energy is stored in rechargeable battery or auxiliary systems that complement the powering of the engine. Power density, cost, and design obstruct their implementation [32]. In their experimental

study of normal city operation, Koyuncy et al. showed that the efficiency of the solar vehicle from solar panel to the vehicle wheel was about 9% [33].

Solar panel–hydrogen FCVs hybrid technology does not refer to the complementary operation of these energy sources, but to the role of solar energy-operated electrolyzers within the energy system to produce feed for the FC [34,35]. Using external hydrogen would also be feasible, but research is focused on the stationary applications of any solar panel–FC combinations [36,37]. It is evident that solar-powered BEVs could be twice as efficient as solar–hydrogen FCVs, because of the energy losses during energy conversion from electricity to hydrogen and then back again. Although direct use in BEVs can be the most efficient use of solar energy, BEVs can have higher life cycle costs than solar–hydrogen FCVs [35].

As can be seen, the current level of technological maturity and the temporary presence of renewable energy make climate-friendly energy sources difficult to integrate into an overall energy system; thus, hybrid solutions usually consist only of two components. The present R&D project, in addition to developing a prototype vehicle, aims to develop software models in which the automatic operation and performance of the energy system demonstrates the potential viability of a novel, multicomponent, autonomous renewable energy system and can be applied to the design of similar hydrogen and renewable systems. The project developed an L5e prototype vehicle, of which there are more than 8 million in worldwide traffic, mostly powered by internal combustion engines. The aim was to combine a mature vehicle design with modern propulsion technology, complemented by a futuristic design. This unique hydrogen-powered, multifunctional vehicle, named Neumann H₂ (Figure 3), has been developed by the John von Neumann University and was presented at the UN Global Climate Change 2023 COP28 conference in the United Arab Emirates, Dubai. The focus of the event was the “Road to Zero” campaign, which aims to make the use of renewable energy sources in the mobility and energy sectors a priority for member states to curb global warming [38]. The Neumann H₂ is a demonstration and research platform. It integrates state-of-the-art energy storage systems, demonstrating the benefits of solar, battery, and hydrogen powertrains.



Figure 3. Digital model of the Neumann H₂ prototype vehicle.

2. Design Principles and Methods

The mutual acceptance of car approvals originally started with the Geneva Agreement of 1958, which covered the United Nations Economic Commission for Europe (UN/ECE).

It was later adopted by other countries and made compulsory. There is currently no “whole vehicle”-type approval in the UN system of regulations. Vehicles can only be approved based on individual specifications and it is up to the contracting parties (countries) to decide which specification is mandatory. The current specifications and their application are set out in UN/ECE/TRANS/WP.29/343 [39].

2.1. Design Principles for Main Parts

L5e vehicles can be divided into two categories. The first is the L5e-A category, which consists mainly of three-wheeled motorcycles and other three-wheeled vehicles designed for passenger transport. The second category is L5e-B, which consists mainly of three-wheeled vehicles for professional use, designed exclusively for the carriage of goods. Two regulatory systems apply to the vehicle type approval process [40].

The electric drive, if it is driven by a multi-phase motor that is not permanently connected to the electric mains, shall be designed to exclude any electrical safety hazards, considering the relevant requirements of UN/ECE Regulation No 100 and ISO 13063 [41,42]. This is also applicable to high voltage components in galvanic contact with the high voltage electrical powertrain. General requirements for on-board diagnostic systems, as defined in Annex IV, point 1.8.1 of Regulation (EU) No 168/2013 [40], require vehicles of categories and subcategories L3e, L4e, L5e-A, and L7e-A to be fitted with an OBD I or OBD II port. This monitors and indicates any circuit or electronic faults in the vehicle’s emission control system that lead to the specified emission thresholds being exceeded and can indicate other faults that are hazardous to road traffic. The steering system of vehicles is considered a critical part of the main components, as it is one of the parts that can affect safety. At an international level, UN/ECE TRANS 79 and, at a European level, EU Directives 91/662/EEC; 92/62/EEC [43–45] contain several specific requirements and test procedures for the steering and cornering of vehicles that have been used during their development.

The braking system of the vehicle must be such that the braking power can be controlled and the driver is able to operate the steering wheel with both hands. The parking brake must also be designed to be adjustable, but it is enough for the driver to hold the steering wheel with only one hand when braking. It can be concluded that the use of the parking brake as a safety brake is accepted and permitted. The parking brake shall be operated only by mechanical components to maintain the holding on a slope.

A report from the National Highway Traffic Safety Administration revealed different risks and hazards for gasoline, natural gas, and hydrogen and highlighted that appropriate engineering controls can ensure the overall desired level of safety for both [46]. Possible sources of danger mostly result from the general structure and operation of the fuel cell vehicle, rather than from the presence of hydrogen [46,47]. Although the lower flammability limit (LFL) of hydrogen is only 4 vol.%, hydrogen does not necessarily ignite spontaneously when released at a high pressure [48]. Liu et al. urged the standard setters to fix conditions for post-accident leakage testing and unify the technical requirements of crash tests of FCVs [49]. Research from the Japan Automobile Research Institute concluded that an accidental leakage and ignition of hydrogen under the wheelbase of a passenger car with the allowable leak rate of 131 NL/min would not have a significant impact on the car or the humans around it [50]. In fact, studies show that the likelihood of ignition above the LFL is heavily dependent on the leakage flow rate, leak time, ventilation, and ignition mechanism [48,50,51]. To minimize risks associated with leaks, the storage and fuel flow management system of Neumann H2 were designed under one enclosure, complying with UN/ECE R 134 standard [52]. The drivetrain of Neumann H2 is designed to deliver category-compliant performance. It is powered by solar panels in addition to hydrogen. A block diagram of this complex powertrain is shown in Figure 4.

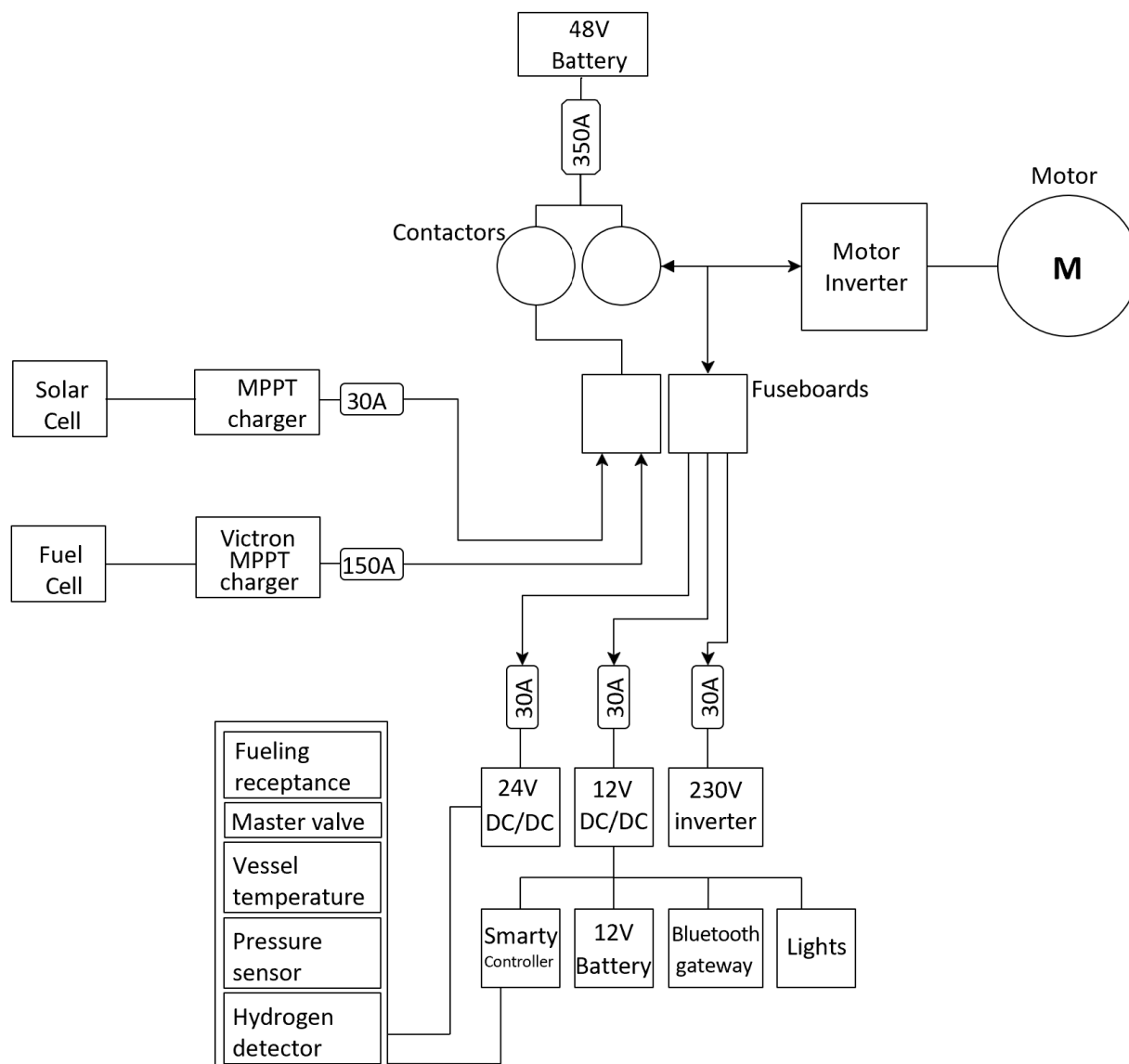


Figure 4. Neumann H2 prototype vehicle powertrain block diagram.

2.2. Artificial Intelligence-Driven Simulation Environment

As can be seen from Figure 4, complex energy management is required for the optimal operation of energy resources. Artificial intelligence is responsible for drive optimization. Furthermore, with the help of AI, the vehicle can also perform environmental recognition using appropriate cameras and image processing algorithms [53–55].

The vehicle has three subsystems, which also declare the three modes of operation, as follows: battery mode, hydrogen mode, and hybrid (solar–battery–hydrogen) propulsion. The systems are complemented by a solar system, which can supply auxiliary systems, like lights or computational units, etc. The system is based on a “Multi-Agent Reinforcement Learning Framework”, where different “Agents” are responsible for different subsystems [53,56,57]. This means that the change between the states of operation will be determined jointly by the Agents.

High-fidelity models were created for the different subsystems (Figure 5). To run the high-fidelity models in real-time in the car itself, Reduced Order Modeling methods were applied and LSTM Networks were trained to replace the high-fidelity models.

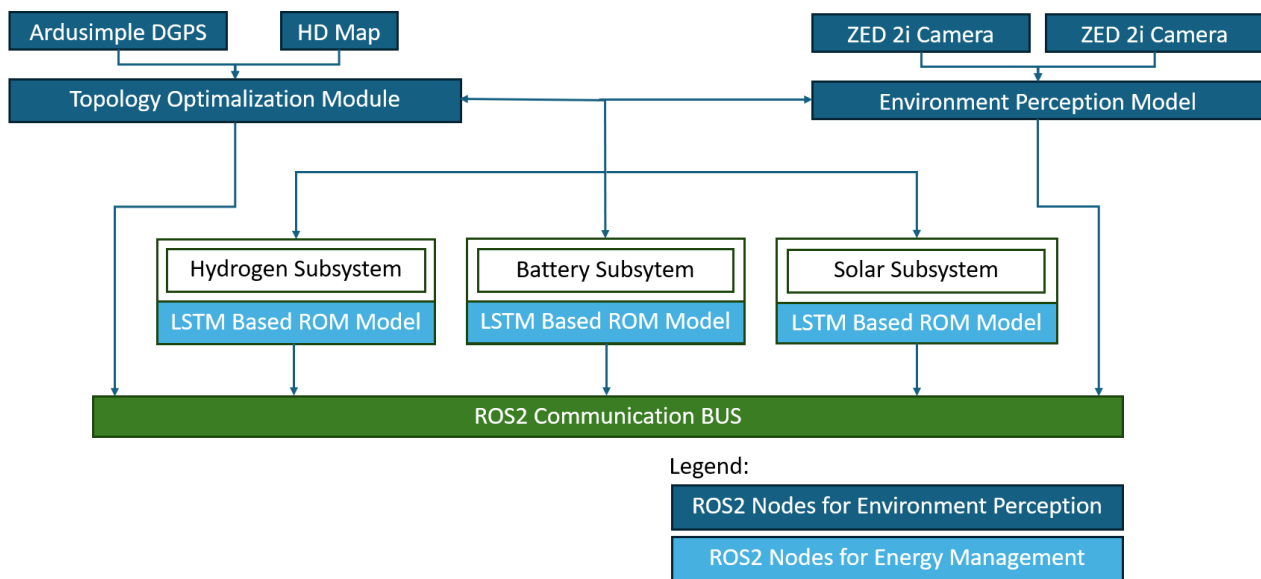


Figure 5. Artificial intelligence-driven system schematic.

The development of the control algorithm was carried out in the MATLAB Simulink/Simscape R2023b simulation environment. The deployment of the neural networks made by MATLAB Compiler SDK to build Docker Images initialize the ROS2 Nodes that contain the different agents. Nvidia Orin was chosen as the central system controller (Main Control Unit—MCU) for the computational platform. The advantage of the hardware next to its computational capability is that the algorithms can be easily deployed directly from MATLAB or by Docker Containers. Since the hardware has enough I/O, there is no obstacle to read and write CAN bus or other protocols; thus, there is no need to introduce additional translation systems between the Control MCU and the MCUs of the subsystems.

3. Results and Discussion

3.1. Structure of the Prototype

The main challenge of the suspension design was to provide the vehicle with the usual handling of passenger cars, by changing it from what is usual for typical three-wheeled vehicles. The 3D model of the manufactured design can be seen in Figure 6. The trail is an important parameter for the self-steering of vehicles, as the higher this value is, the greater the force that will keep the wheels straight. However, as the value increases, the force to steer away from the straight line also increases. The camber angle determines the traction of the wheel. The steering angle affects the turning circle of the vehicle. The larger the steering angle, the smaller the arc the vehicle can turn. Due to the one-sided suspension, the steering angle is 30 degrees symmetrically per side, which is less than that of a standard vehicle of the same size. The turning radius of the vehicle with the chassis geometry used is 12.1 m. The rear wheel inclination is -0.83 degrees when the wheel is in the unloaded position and -1.33 degrees when fully loaded. This means a -0.5 degree wheel angle change, which significantly improves vehicle stability when cornering. By parameterizing the swingarms, another very important chassis geometry adjustment can be achieved, called wheel alignment. The degree of wheel compliance is important for the steerability of a vehicle, as it can improve the straight-line stability of a vehicle to a large extent.

The braking system must provide a deceleration of at least 5.8 m/s^2 according to the EGB 13 standard [58] and has been installed in the vehicle accordingly. The cargo floor can be loaded with two standardized pallets placed in a row to provide the intended functions (Figure 7).

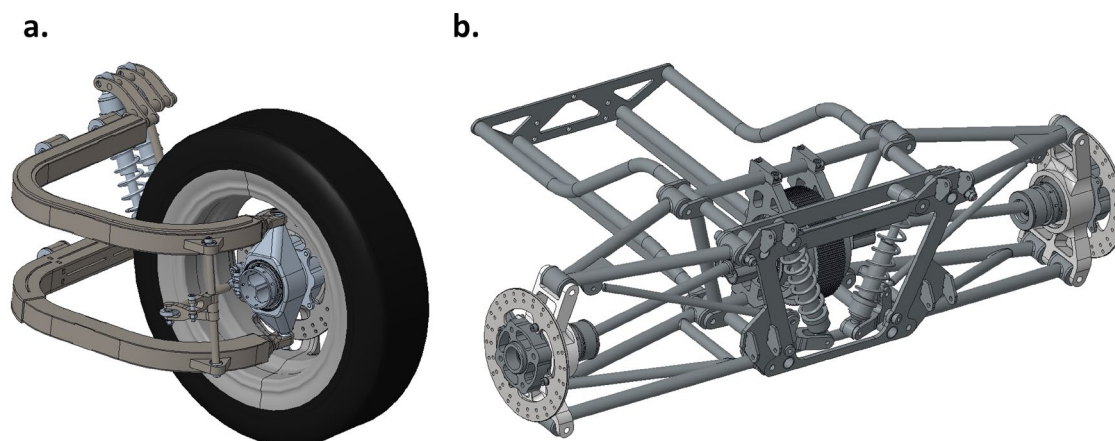


Figure 6. The front (a) and rear (b) chassis of the vehicle.

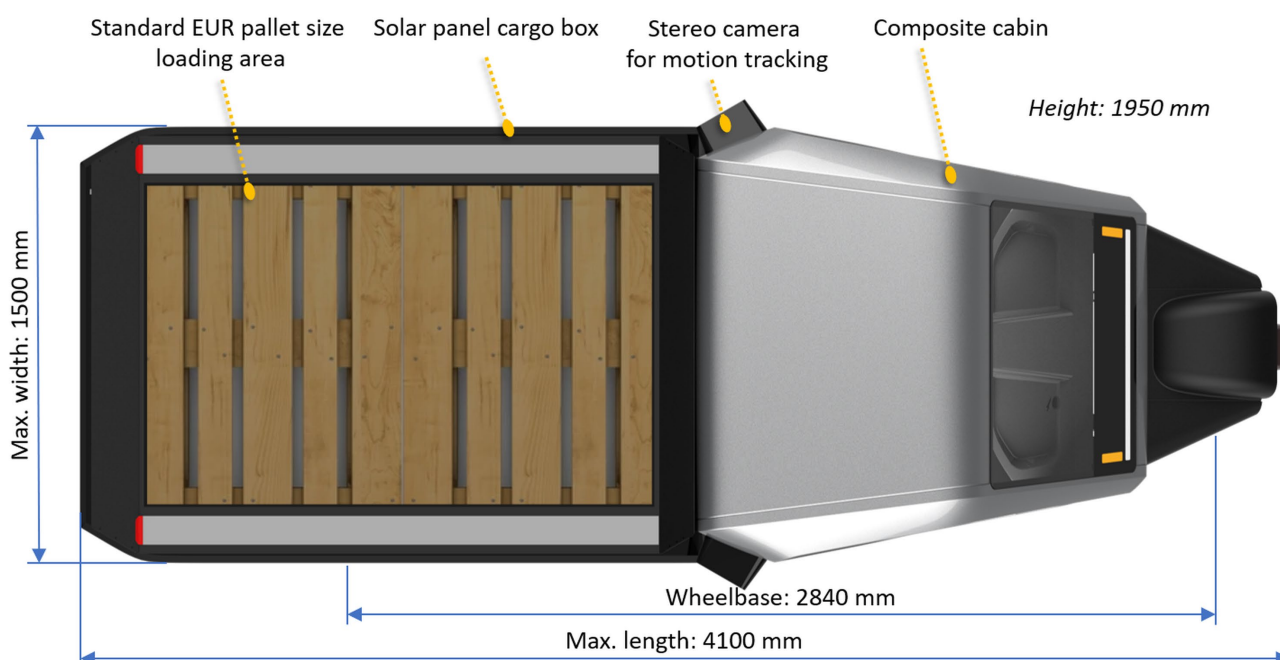


Figure 7. Main dimensions of the Neumann H2.

The battery pack is a self-made lithium-ion type with a capacity of 4100 Wh and a mass of 28 kg, which includes the case and Battery Management System (BMS). The nominal voltage is 44.4 V, maximum voltage is 49.8 V, and minimum voltage is 32.4 V. The chosen electric motor type is an Engiro 205 A, with a nominal power of 11 kW. It is an air-cooled, permanent magnet synchronous motor with a voltage range from 48 V to 200 V. The cargo box is covered with 3 Longi Solar LR5-54HIB 405 Wp solar panels. The combined power is 1200 Wp.

On the side of the composite cabin, the prototype has two ZED 2i cameras which offer CUDA acceleration, leveraging the power of the used NVIDIA Orin GPU to accelerate depth computation and object detection. The prototype vehicle produced and its interior surfaces are shown in Figure 8.



Figure 8. The built Neumann H2 prototype vehicle.

3.2. Hydrogen Storage, Fuel Delivery, and Fuel Cell Subsystems

Hydrogen accumulation in the cylinder enclosure is monitored by a hydrogen detector that is located above the hydrogen container. Interestingly, international standards differ in the alarm threshold of the hydrogen detector. For example, Chinese national standards specify to alarm the driver when the internal hydrogen concentration reaches 2 vol.% and to shut down the gas supply when 3 vol.% is reached [59]. However, the Road Transport Vehicle Act of Japan and UN/ECE R 134 standard valid in the EU sets the threshold for alarms at 4 vol.% [47,50,52]. The alarm threshold in Neumann H2 is set at 2 vol.% and gas supply shut-off is at 4 vol.%. The parts are included in the fuel system, which is shown in the flow diagram in Figure 9.

The C1-31316-X1-type (WEH GmbH, Illertissen, Germany) fueling receptacle fits the SAE J2600:201510 standard, making the car compatible with public fueling stations [60]. The fill line is well protected from reverse flow, as the fueling receptacle and the shut-off valve both act as check valves. This is further strengthened by the dedicated check valve between the receptacle and the hydrogen tank valve. Possible contamination in hydrogen gas is filtered in two places. First, in the fill line, the fueling receptacle includes a 50 micron filter, which is followed by a 0.1 micron high-capacity coalescing filter. Second, the supply line of the fuel cell is protected from possible debris coming from any component behind it with a 7 micron tee-type filter.

An L028-type (Luxfer Gas Cylinders Ltd., Nottingham, UK) composite overwrapped pressure vessel with a seamless aluminum alloy liner was used for fuel storage. This type of gas cylinder is called type 3, with the specifications of 28 L water volume, 350 bar nominal working pressure, and a capacity of 0.7 kg of stored hydrogen. The storage tank was type approved according to the EC 79 standard, which has since been withdrawn, but meets

the requirements of the R134 standard in force [52,61]. The tank valve is mounted directly on the container that integrates an excess flow valve, a manual and a solenoid shut-off valve, a bleed valve, a thermally activated pressure relief device, a pressure transmitter, and a temperature transmitter. All electrical devices (e.g., solenoids, transmitters) and their connections comply to the ATEX standard [62]. The live port of the tank valve that is directly connected to the cylinder was used to connect a high-pressure relief valve set to 380 bar and a high-pressure emergency venting solenoid. This solenoid is an extra accessory that is not part of the standard hydrogen system, but it can justify the defueling of the fuel system by the pilot in case of emergency resulting from the prototype nature of the vehicle. The emergency venting solenoid is independently powered by a 48 V backup circuit to make its activation possible even if the main circuit is shut-off.

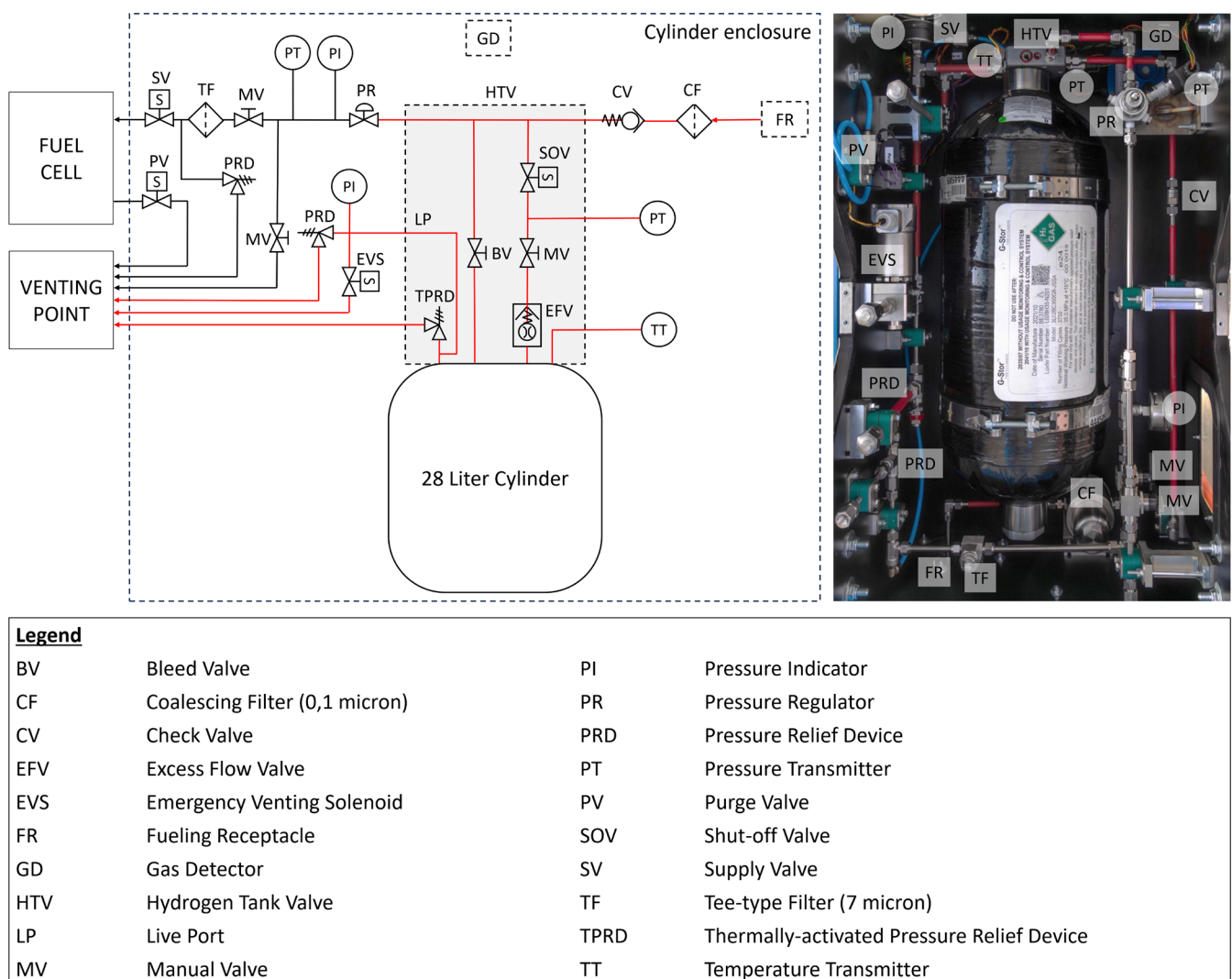


Figure 9. P&ID of the fuel system (high pressure fuel lines are marked with red, low pressure fuel lines are uncolored).

The output port of the tank valve continues in an LW-TS414-type (Pressure Tech Ltd., Derbyshire, UK) two-stage pressure regulator that reduces the inlet pressure to a stable 0.5 bar, which is the operating pressure of the fuel cell unit. The fuel cell is protected from overpressure with a low-pressure relief device set to 0.7 bar. Two manual valves are placed on the low-pressure line. One can insulate the fuel system in case of fuel cell maintenance and one can be used to discharge hydrogen from the low-pressure port for the sake of safe replacement of the gas cylinder. Solenoid valves on low-pressure fuel lines are responsible

for supplying and purging hydrogen gas. Unused hydrogen is released to the environment and is not recirculated to the anode inlet, but this will be later optimized [63,64].

As the main power source of the Neumann H2, a Horizon H-5000-type open-cathode Polymer Electrolyte Membrane (PEM) fuel cell was chosen. The reason of choice was that this system offers the smallest number of peripherals, which was a main concern during the design. The nominal power output of the stack is 5000 W (72 V at 70 A), running on 99.995 vol.% pure H₂ gas. The cathode air supply is provided by four fan blowers, which are both responsible for supplying oxygen and cooling the stack at its nominal temperature of 65 °C. Air is aspirated through an airbox, which includes a cathode air filter that catches gases that can poison the catalyst in the fuel cell. The complete drivetrain is shown in Figure 10.

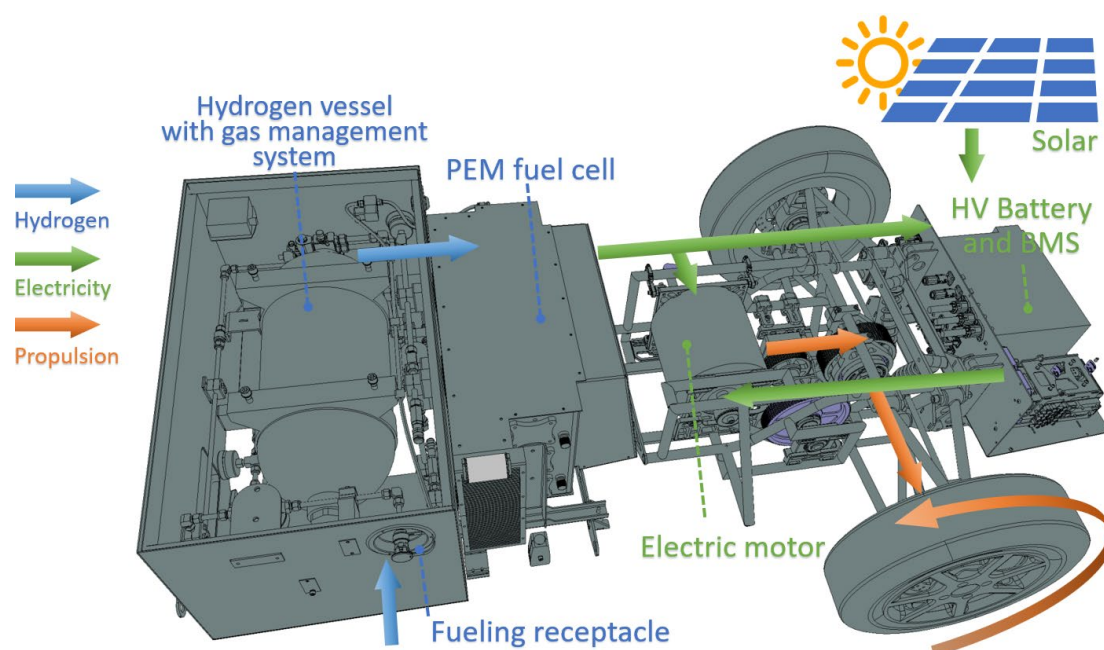


Figure 10. Neumann H2 hydrogen fuel cell electric vehicle powertrain system.

3.3. Artificial Intelligence-Driven Energy Management System

MathWorks' fuel cell electric vehicle reference model [54] was utilized as the basic model for development. A barrier to real-time energy management systems is the runtime of the model (Figure 11). By profiling the solution, the most time-consuming module is the Electric Plant that includes the simulation of fuel cell, battery module, etc.

To reduce computational time, a Reduced Order Modeling method was applied to the Electric Plant. An LSTM network was trained for both the input and output of the Electric Plant. The dataset was generated based on the WLTP Class 1 cycle (Figure 12).

Various neural network architectures with different numbers of hidden layers were employed between 10 and 1000, with spacing of 10. Training of the LSTM Network happened with the following hyperparameters on Nvidia RTX4090 (Table 1).

In terms of performance and accuracy, the following architecture proved to be the best (Table 2).

Deploying a relatively small and shallow network allowed us to accelerate the running time, reducing the total time from 27.601 to 0.042 s. It means that by deploying that LSTM network to Nvidia Orin, it is capable to run in real-time. The dataset contains the following inputs and outputs (Table 3) that were used for training the neural network. The comparison of the simulated and the predicted current of the fuel cell based on the ROM method is shown in Figure 13.

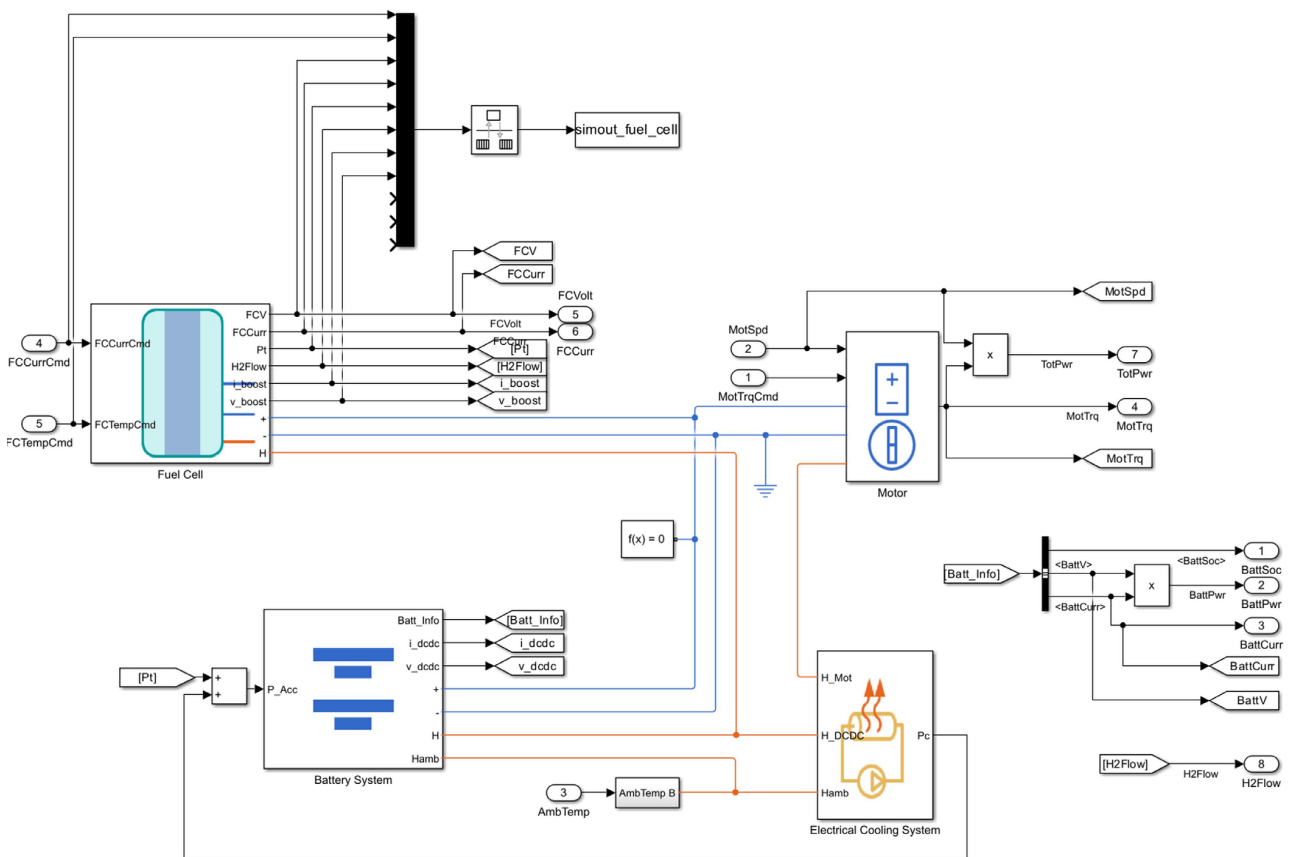
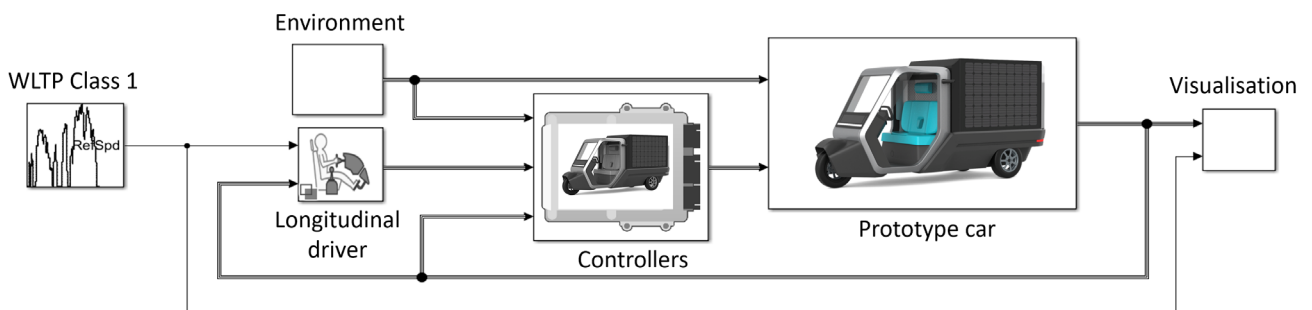


Figure 11. MathWorks' Electrical Plant of fuel cell vehicles [65].



Aim:

- Analyze Power and Energy
- Generate Mapped Fuel Cell from Spreadsheet

Figure 12. MathWorks' WLTP cycle for fuel cell electric vehicle: a schematic model [65].

Table 1. LSTM Network Training Hyperparameters.

#	Hyperparameters	Setup
1	Number of Epoch	1×10^5
2	Gradient Threshold	1
3	Initial Learning Rate	5×10^{-3}
4	Learning Rate Schedule	Piecewise
5	Learning Rate Drop Period	1×10^4
6	Learning Rate Drop Factor	0.6

Table 2. The applied neural network architecture with different numbers of hidden layers.

#	Name	Type	Activations	Learnable	States	
1	sequenceinput Sequence input with 5 dims.	Sequence Input	$5(C) \times 1(B) \times 1(T)$	-	-	
2	fc_1 800 fully connected layers	Fully connected	$800(C) \times 1(B) \times 1(T)$	Weights Bias	800×5 800×1	-
3	relu_1 ReLU	ReLU	$800(C) \times 1(B) \times 1(T)$	-	-	
4	1stm_1 LSTM with 800 hidden units	LSTM	$800(C) \times 1(B) \times 1(T)$	Input Weight Recurrent Bias	3200×800 3200×800 3200×1	Hidden State Cell State
5	1 stm_2 LSTM with 800 hidden units	LSTM	$800(C) \times 1(B) \times 1(T)$	Input Weight Recurrent Bias	3200×800 3200×800 3200×1	Hidden State Cell State
6	relu_1 ReLU	ReLU	$800(C) \times 1(B) \times 1(T)$	-	-	
7	fc_2 8 fully connected layers	Fully Connected	$8(C) \times 1(B) \times 1(T)$	Weight Bias	8×800 8×1	-
8	regression output means-squared-error	Regression Output	$8(C) \times 1(B) \times 1(T)$	-	-	

Table 3. The input and output signals of the ROM model with model accuracy prediction.

Input Signal of ROM Model	Output Signal of ROM Model	ROM Model Accuracy Predicting
Motor Torque Command	Battery State of Charge [%]	88%
Motor Speed [RPM]	Battery Power [W]	96%
Ambient Temperature [K]	Battery Current [A]	92%
Fuel Cell Temperature Command	Motor Torque [Nm]	98%
Fuel Cell Current Command	Fuel Cell Voltage [V]	94%
	Fuel Cell Current [A]	94%
	Total Power [W]	91%
	H2 Flow [kg/s]	70%

3.4. Deep Learning for Environment Recognition

Two ZED2i stereo cameras, Nvidia Orin, and two displays, along with the necessary software environments, were used for the environment perception model. From the software side, ZED SDK 4.0, Python 3.11.2, and the default Linux (Ubuntu 22.04.02 LTS) features (bash scripts, services, etc.) were used in this project. The A2D2 Dataset [66] was used for training, along with the ResNet18 layers architecture. The input received 512×512 images. The environmental detection is shown in Figure 14.

The system's desired behavior has the following rules:

- The viewer must be full screen.
- The viewer must start on system boot-up.
- In case of any issue with the USB connection, the program tries to restart itself.
- Both displays must be in lain orientation with the corresponding viewer windows.

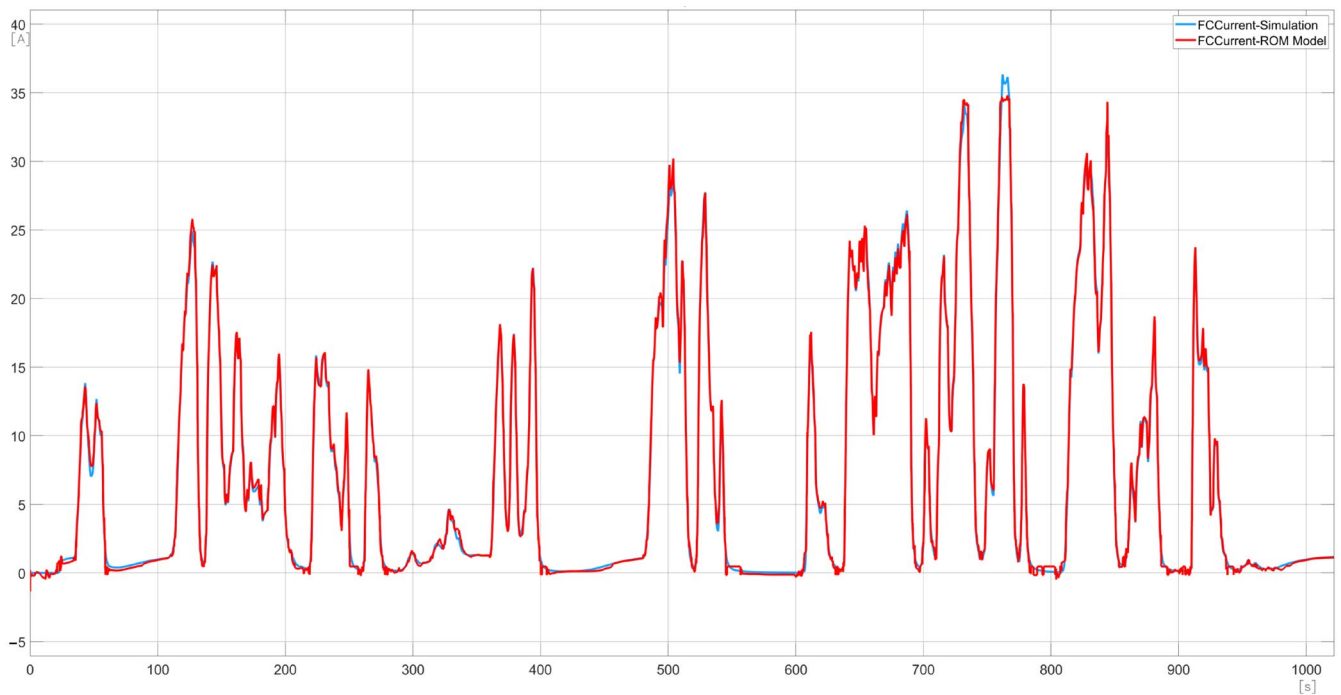


Figure 13. Comparison of simulated (blue line) and the predicted (red line) current of the fuel cell, based on the ROM method.



Figure 14. The process of environment detection on the vehicle.

4. Conclusions

Being inspired by the technical challenges in the field of green powertrains, we report a study on the technical feasibility of an AI-controlled complex solar panel–hydrogen FC–battery energy system, embodied as the Neumann H2 L5e vehicle. Feasibility was demonstrated for a double wishbone chassis, with a 5 kW PEM fuel cell as the primary power source, as well as 0.7 kg of stored hydrogen in one 350 bar type 3 compressed gaseous cylinder. The fuel system was built in one enclosure with the cylinder, according to the R 134 standard. The energy system is supplemented by 1200 Wp from solar panels, which can provide propulsion and supply auxiliary systems through a lithium-ion battery with a capacity of 4100 Wh. The energy system is controlled by an artificial intelligence-based system, which enables a range of 250 km with a maximum speed of 60 km/h. Overall,

this study found it feasible to design, build, and operate a three-wheeled vehicle powered by a combination of hydrogen fuel cells and solar panels, thus providing a real, user-friendly R&D platform for the development of combined climate-friendly energy system constructions in mobility.

Author Contributions: Conceptualization, K.K. and E.V.; methodology, K.K., L.S. and D.I.K.; software, L.S.; validation, K.K., L.S. and D.I.K.; formal analysis, K.K. and E.V.; investigation, K.K., L.S. and D.I.K.; resources, K.K.; data curation, L.S.; writing—original draft preparation, K.K.; writing—review and editing, K.K. and E.V.; visualization, K.K. and E.V.; supervision, E.V.; project administration, K.K.; funding acquisition, K.K. All authors have read and agreed to the published version of the manuscript.

Funding: John von Neumann University Foundation RDI grant.

Data Availability Statement: The data presented in this study are available on request from the corresponding author. The data are not publicly available due to restrictions imposed by the funding to ensure compliance with data usage agreements.

Acknowledgments: This work was supported by the National Laboratory for Renewable Energy (Project no. RRF-2.3.1-21-2022-00009), which has been implemented with the support provided by the Recovery and Resilience Facility of the European Union within the framework of Programme Széchenyi Plan Plus, Hungary.

Conflicts of Interest: The authors declare no conflicts of interest.

References

1. U.S. Energy Information Administration (EIA). *Monthly Energy Review May 2023*; EIA: Washington, DC, USA, 2023.
2. Davis, S.C.; Diegel, S.W.; Boundy, R.G. *Transportation Energy Data Book*, 31st ed.; Oak Ridge National Laboratory (ORNL): Oak Ridge, TN, USA, 2012.
3. IEA. *CO₂ Emissions from Fuel Combustion*; IEA: Paris, France, 2013. [[CrossRef](#)]
4. Zefreh, M.M.; Torok, A. Theoretical Comparison of the Effects of Different Traffic Conditions on Urban Road Environmental External Costs. *Sustainability* **2021**, *13*, 3541. [[CrossRef](#)]
5. Kondor, I.P.; Zöldy, M.; Mihály, D. Experimental Investigation on the Performance and Emission Characteristics of a Compression Ignition Engine Using Waste-Based Tire Pyrolysis Fuel and Diesel Fuel Blends. *Energies* **2021**, *14*, 7903. [[CrossRef](#)]
6. Zöldy, M.; Kondor, I.P. Simulation and Injector Bench Test Validation of Different Nozzle Hole Effect on Pyrolysis Oil-Diesel Oil Mixtures. *Energies* **2021**, *14*, 2396. [[CrossRef](#)]
7. Murgia, F. P-Block Elements as Negative Electrode Materials for Magnesium-Ion Batteries: Electrochemical Mechanism and Performance. Ph.D. Thesis, Université Montpellier, Montpellier, France, 2016.
8. Shafiee, S.; Topal, E. When Will Fossil Fuel Reserves Be Diminished? *Energy Policy* **2009**, *37*, 181–189. [[CrossRef](#)]
9. Laimon, M.; Yusaf, T. Towards Energy Freedom: Exploring Sustainable Solutions for Energy Independence and Self-Sufficiency Using Integrated Renewable Energy-Driven Hydrogen System. *Renew. Energy* **2024**, *222*, 119948. [[CrossRef](#)]
10. Baharudin, L.; Watson, M. Hydrogen Applications and Research Activities in Its Production Routes through Catalytic Hydrocarbon Conversion. *Rev. Chem. Eng.* **2017**, *34*, 43–72. [[CrossRef](#)]
11. Hosseini, S.E.; Butler, B. An Overview of Development and Challenges in Hydrogen Powered Vehicles. *Int. J. Green Energy* **2019**, *17*, 13–37. [[CrossRef](#)]
12. Suleman, F.; Dincer, I.; Agelin-Chaab, M. Environmental Impact Assessment and Comparison of Some Hydrogen Production Options. *Int. J. Hydrogen Energy* **2015**, *40*, 6976–6987. [[CrossRef](#)]
13. IEA. *Global Hydrogen Review 2023*; IEA: Paris, France, 2023.
14. Dincer, I.; Acar, C. Review and Evaluation of Hydrogen Production Methods for Better Sustainability. *Int. J. Hydrogen Energy* **2015**, *40*, 11094–11111. [[CrossRef](#)]
15. IEA. *The Future of Hydrogen: Seizing Today's Opportunities*; OECD: Paris, France, 2019. [[CrossRef](#)]
16. Kis, D.I.; Kókai, E. A Review on the Factors of Liner Collapse in Type IV Hydrogen Storage Vessels. *Int. J. Hydrogen Energy* **2023**, *50*, 236–253. [[CrossRef](#)]
17. Gómez, J.A.; Santos, D.M.F. The Status of On-Board Hydrogen Storage in Fuel Cell Electric Vehicles. *Designs* **2023**, *7*, 97. [[CrossRef](#)]
18. Castillo Campo, O.; Alvarez Fernandez, R.; Domingo, R. Opportunities and Barriers of Hydrogen–Electric Hybrid Powertrain Vans: A Systematic Literature Review. *Processes* **2020**, *8*, 1261. [[CrossRef](#)]
19. Gis, W. Ecological and Functional Aspects of Operation of Electric Vehicles With Fuel Cell. *J. KONBiN* **2020**, *50*, 165–176. [[CrossRef](#)]
20. Pielecha, I.; Cieslik, W.; Andrzej, S. The Use of Electric Drive in Urban Driving Conditions Using a Hydrogen Powered Vehicle—Toyota Mirai. *Combust. Engines* **2018**, *172*, 51–58. [[CrossRef](#)]
21. Vodovozov, V.; Raud, Z.; Petlenkov, E. Review of Energy Challenges and Horizons of Hydrogen City Buses. *Energies* **2022**, *15*, 6945. [[CrossRef](#)]

22. Alves, M.P.; Gul, W.; Cimini Junior, C.A.; Ha, S.K. A Review on Industrial Perspectives and Challenges on Material, Manufacturing, Design and Development of Compressed Hydrogen Storage Tanks for the Transportation Sector. *Energies* **2022**, *15*, 5152. [CrossRef]
23. Binder, M. *Clean Urban Transport for Europe Project Final Report*; EU Commission: Brussels, Belgium, 2006.
24. Stolzenburg, K.; Whitehouse, N.; Whitehouse, S. *JIVE D3.24/JIVE 2 D3.7 Best Practice Report*; EU Commission: Brussels, Belgium, 2020.
25. IEA. *Global EV Outlook 2023*; IEA: Paris, France, 2023.
26. Li, H.; Guo, H.; Yousefi, N. A Hybrid Fuel Cell/Battery Vehicle by Considering Economy Considerations Optimized by Converged Barnacles Mating Optimizer (CBMO) Algorithm. *Energy Rep.* **2020**, *6*, 2441–2449. [CrossRef]
27. Yu, P.; Li, M.; Wang, Y.; Chen, Z. Fuel Cell Hybrid Electric Vehicles: A Review of Topologies and Energy Management Strategies. *World Electr. Veh. J.* **2022**, *13*, 172. [CrossRef]
28. Ragab, A.; Marei, M.I.; Mokhtar, M. Comprehensive Study of Fuel Cell Hybrid Electric Vehicles: Classification, Topologies, and Control System Comparisons. *Appl. Sci.* **2023**, *13*, 13057. [CrossRef]
29. Ferrara, A.; Okoli, M.; Jakubek, S.; Hametner, C. Energy Management of Heavy-Duty Fuel Cell Electric Vehicles: Model Predictive Control for Fuel Consumption and Lifetime Optimization. *IFAC-PapersOnLine* **2020**, *53*, 14205–14210. [CrossRef]
30. Wang, W.; Hao, Z.; Qu, F.; Li, W.; Wu, L.; Li, X.; Wang, P.; Ma, Y. Review of Energy Management Methods for Fuel Cell Vehicles: From the Perspective of Driving Cycle Information. *Sensors* **2023**, *23*, 8571. [CrossRef]
31. Romero, O.; Miura, A.S.; Parra, L.; Lloret, J. Low-Cost System for Automatic Recognition of Driving Pattern in Assessing Interurban Mobility Using Geo-Information. *ISPRS Int. J. Geoinf.* **2022**, *11*, 597. [CrossRef]
32. Babalola, P.O.; Atiba, O.E. Solar Powered Cars—A Review. *IOP Conf. Ser. Mater. Sci. Eng.* **2021**, *1107*, 012058. [CrossRef]
33. Koyuncu, T. Practical Efficiency of Photovoltaic Panel Used for Solar Vehicles. In *IOP Conference Series: Earth and Environmental Science*; Institute of Physics Publishing: Bristol, UK, 2017; Volume 83.
34. Yilanci, A.; Dincer, I.; Ozturk, H. A Review on Solar-Hydrogen/Fuel Cell Hybrid Energy Systems for Stationary Applications. *Prog. Energy Combust. Sci.* **2009**, *35*, 231–244. [CrossRef]
35. DeLuchi, M.A.; Ogden, J.M. Solar-Hydrogen Fuel-Cell Vehicles. *Transp. Res. Part A Policy Pract.* **1993**, *27*, 255–275. [CrossRef]
36. Felseghi, R.-A.; Aşchilean, I.; Cobîrzan, N.; Bolboacă, A.M.; Raboaca, M.S. Optimal Synergy between Photovoltaic Panels and Hydrogen Fuel Cells for Green Power Supply of a Green Building—A Case Study. *Sustainability* **2021**, *13*, 6304. [CrossRef]
37. Zhang, F.; Wang, B.; Gong, Z.; Zhang, X.; Qin, Z.; Jiao, K. Development of Photovoltaic-Electrolyzer-Fuel Cell System for Hydrogen Production and Power Generation. *Energy* **2023**, *263*, 125566. [CrossRef]
38. Muratori, M.; Borlaug, B.; Ledna, C.; Jadun, P.; Kailas, A. Road to Zero: Research and Industry Perspectives on Zero-Emission Commercial Vehicles. *iScience* **2023**, *26*, 106751. [CrossRef]
39. UNECE. Agreement Concerning the Adoption of Harmonized Technical United Nations Regulations for Wheeled Vehicles, Equipment and Parts Which Can Be Fitted and/or Be Used on Wheeled Vehicles and the Conditions for Reciprocal Recognition of Approvals Granted on the Basis of These United Nations Regulations. 2022. Available online: https://treaties.un.org/Pages/ViewDetails.aspx?src=IND&mtdsg_no=XI-B-16&chapter=11&clang=_en (accessed on 4 February 2024).
40. European Parliament, Council of the European Union. Regulation (EU) No 168/2013 of the European Parliament and of the Council of 15 January 2013 on the Approval and Market Surveillance of Two- or Three-Wheel Vehicles and Quadricycles Text with EEA Relevance 2020. Available online: <https://eur-lex.europa.eu/legal-content/EN/ALL/?uri=celex:32013R0168> (accessed on 4 February 2024).
41. Regulation No. 100: Uniform Provisions Concerning the Approval of Vehicles with Regard to Specific Requirements for the Electric Power Train. 2022. Available online: [https://eur-lex.europa.eu/legal-content/EN/TXT/?uri=CELEX:42011X0302\(01\)](https://eur-lex.europa.eu/legal-content/EN/TXT/?uri=CELEX:42011X0302(01)) (accessed on 4 February 2024).
42. ISO 13063; Electrically Propelled Mopeds and Motorcycles. International Organization for Standardization: Geneva, Switzerland, 2012.
43. European Commission Commission Directive 92/62/EEC of 2 July 1992 Adapting to Technical Progress Council Directive 70/311/EEC Relating to Steering Equipment for Motor Vehicles and Their Trailers. 1992. Available online: <https://eur-lex.europa.eu/legal-content/EN/TXT/?uri=celex:31992L0062> (accessed on 4 February 2024).
44. European Commission Commission Directive 91/662/EEC of 6 December 1991 Adapting to Technical Progress Council Directive 74/297/EEC in Respect of the Behaviour of the Steering Wheel and Column in an Impact 1991. Available online: <https://eur-lex.europa.eu/legal-content/EN/ALL/?uri=celex:31991L0662> (accessed on 4 February 2024).
45. UN/ECE/TRANS/Regulation No. 79-01; Uniform Provisions Concerning the Approval of: Vehicles with Regard to Steering Equipment. 1988. Available online: <https://www.interregs.com/catalogue/details/ece-79/regulation-no-79-01/steering-equipment/> (accessed on 4 February 2024).
46. National Highway Traffic Safety Administration. *Failure Modes and Effects Analysis for Hydrogen Fuel Cell Vehicles—Subtask 1*; NHTSA: Washington, DC, USA, 2009.
47. Flamberg, S.; Rose, S.; Stephens, D. *Analysis of Published Hydrogen Vehicle Safety Research*; United States National Highway Traffic Safety Administration: Washington, DC, USA, 2010.
48. Astbury, G.; Hawksworth, S. Spontaneous Ignition of Hydrogen Leaks: A Review of Postulated Mechanisms. *Int. J. Hydrogen Energy* **2007**, *32*, 2178–2185. [CrossRef]

49. Liu, M.; Zhang, S. Research on Hydrogen Fuel Cell Safety Detection Analysis Based on Leakage Quality Limit Detection Method. *J. Phys. Conf. Ser.* **2022**, *2174*, 012049. [CrossRef]
50. Maeda, Y.; Takahashi, M.; Tamura, Y.; Suzuki, J.; Watanabe, S. *Test of Vehicle Ignition Due to Hydrogen Gas Leakage*; SAE International: Warrendale, PA, USA, 2006.
51. Liu, W.; Christopher, D.M. Dispersion of Hydrogen Leaking from a Hydrogen Fuel Cell Vehicle. *Int. J. Hydrogen Energy* **2015**, *40*, 16673–16682. [CrossRef]
52. Regulation No 134 of the Economic Commission for Europe of the United Nations (UN/ECE) Uniform Provisions Concerning the Approval of Motor Vehicles and Their Components with Regard to the Safety-Related Performance of Hydrogen-Fuelled Vehicles (HFCV) 2019. Available online: <https://op.europa.eu/en/publication-detail/-/publication/8aad3d19-7870-11e9-9f05-01aa75ed71a1/language-en> (accessed on 4 February 2024).
53. Snoussi, J.; Ben Elghali, S.; Benbouzid, M.; Mimouni, M. Auto-Adaptive Filtering-Based Energy Management Strategy for Fuel Cell Hybrid Electric Vehicles. *Energies* **2018**, *11*, 2118. [CrossRef]
54. Liu, Y.; Liang, J.; Song, J.; Ye, J. Research on Energy Management Strategy of Fuel Cell Vehicle Based on Multi-Dimensional Dynamic Programming. *Energies* **2022**, *15*, 5190. [CrossRef]
55. Tornai, K.; Oláh, A.; Drenyovszki, R.; Kovács, L.; Pinté, I.; Levendovszky, J. Recurrent Neural Network Based User Classification for Smart Grids. In Proceedings of the 2017 IEEE Power & Energy Society Innovative Smart Grid Technologies Conference (ISGT), Washington, DC, USA, 23–26 April 2017; pp. 1–5.
56. Johanyak, Z.C.; Tikk, D.; Kovacs, S.; Wong, K.W. Fuzzy Rule Interpolation Matlab Toolbox—FRI Toolbox. In Proceedings of the 2006 IEEE International Conference on Fuzzy Systems, Vancouver, BC, Canada, 16–21 July 2006; pp. 351–357.
57. Tornai, K.; Kovács, L.; Oláh, A.; Drenyovszki, R.; Pintér, I.; Tisza, D.; Levendovszky, J. Classification for Consumption Data in Smart Grid Based on Forecasting Time Series. *Electr. Power Syst. Res.* **2016**, *141*, 191–201. [CrossRef]
58. European Parliament, Council of the European Union. Regulation No 13 of the Economic Commission for Europe of the United Nations (UN/ECE)—Uniform Provisions Concerning the Approval of Vehicles of Categories M, N and O with Regard to Braking [2016/194]. 2015. Available online: <https://op.europa.eu/en/publication-detail/-/publication/0a43f880-d612-11e5-a4b5-01aa75ed71a1/language-en> (accessed on 4 February 2024).
59. *GB/T 24549-2020*; Fuel Cell Electric Vehicles—Safety Requirements. Standardization Administration of China: Beijing, China, 2020.
60. *SAE J2600_201510*; Compressed Hydrogen Surface Vehicle Fueling Connection Devices. SAE International: Warrendale, PA, USA, 2015.
61. Regulation (EC) No 79/2009 of the European Parliament and of the Council of 14 January 2009 on Type-Approval of Hydrogen-Powered Motor Vehicles, and Amending Directive 2007/46/EC 2009. Available online: <https://eur-lex.europa.eu/legal-content/EN/TXT/HTML/?uri=CELEX:32009R0079> (accessed on 4 February 2024).
62. European Commission. *Atex Guidelines*, 4th ed.; European Commission: Brussels, Belgium, 2012.
63. Wiebe, W.; Unwerth, T.V.; Schmitz, S. Hydrogen Pump for Hydrogen Recirculation in Fuel Cell Vehicles. *E3S Web Conf.* **2020**, *155*, 01001. [CrossRef]
64. Shi, L.; Tang, X.; Xu, S.; Zheng, M. Comprehensive Analysis of Shutdown Purge Influencing Factors of Proton Exchange Membrane Fuel Cell Based on Water Heat Transfer and Water Vapor Phase Change Mechanism. *Appl. Therm. Eng.* **2024**, *239*, 122175. [CrossRef]
65. FCEV Reference Application. Available online: <https://www.mathworks.com/help/autoblks/ug/fuel-cell-electric-vehicle-reference-application.html> (accessed on 4 February 2024).
66. Dataset. Available online: <https://www.a2d2.audi/a2d2/en/dataset.html> (accessed on 4 February 2024).

Disclaimer/Publisher’s Note: The statements, opinions and data contained in all publications are solely those of the individual author(s) and contributor(s) and not of MDPI and/or the editor(s). MDPI and/or the editor(s) disclaim responsibility for any injury to people or property resulting from any ideas, methods, instructions or products referred to in the content.